Valproate attenuates diabetic nephropathy through inhibition of endoplasmic reticulum stress-induced apoptosis

XIN-YI SUN[1,2], HAN-JIAO QIN[3], ZE ZHANG[4], YE XU[5], XIAO-CHUN YANG[1], DONG-MING ZHAO[2], XIAO-NING LI[1] and LIAN-KUN SUN[1]

[1]Department of Pathophysiology, Basic College of Medicine, Jilin University, Changchun, Jilin 130021; [2]Department of Endocrinology and Metabolism, Affiliated Hospital of Beihua University, Changchun, Jilin 132011; [3]Department of Endocrinology and Metabolism, First Clinical Hospital of Norman Bethune College of Medicine; [4]Department of Clinical Medicine, Norman Bethune Health Science Center, Jilin University, Changchun, Jilin 130021; [5]Department of Histology and Embryology, Medical Research Laboratory, Jilin Medical College, Changchun, Jilin 132013, P.R. China

Received December 12, 2014; Accepted October 6, 2015

DOI: 10.3892/mmr.2015.4580

Abstract. Previous studies have suggested that endoplasmic reticulum stress (ERS) is one of the mechanisms responsible for the pathogenesis of diabetic nephropathy (DN). Histone acetylation modification can regulate the transcription of genes and is involved in the regulation of ERS. Valproate (VPA), a nonselective histone deacetylase inhibitor, has been reported to have a protective role in kidney tissue injury, however, whether VPA can prevent DN remains to be elucidated. In the present study, it was found that VPA increases the expression of glucose-regulated protein (GRP78) and reduces the protein expression of C/EBP-homologous protein (CHOP), growth arrest and DNA-damage-inducible gene 153 and caspase-12 in a rat model of DN. VPA can reduce renal cell apoptosis and alleviate proteinuria and alterations in serum creatinine. VPA also upregulates the acetylation level of histone H4 in the promoter of GRP78 and downregulates the acetylation level of histone H4 in the promoter of CHOP. Collectively, the data indicate that VPA can relieve ERS and reduce renal cell apoptosis, and thus attenuate renal injury in a rat model of DN by regulating the acetylation level of histone H4 in ERS-associated protein promoters.

Introduction

Diabetic nephropathy (DN) is a severe complication of diabetes mellitus and is the major cause of end-stage renal disease (1,2) Since the pathogenesis of DN remains to be elucidated, there is currently no effective treatment. Traditionally, it was hypothesized that glucose metabolism, renal hemodynamics, oxidative stress, cytokines and genetic factors were involved in the pathogenesis of DN (3). Previous studies have found that numerous factors, including excess nutrients and free fatty acids, high glucose, and oxidative stress in the diabetic condition can cause endoplasmic reticulum stress (ERS) and initiate proapoptotic pathways inducing apoptosis and tissue damage (4,5). Thus, ERS is one mechanism responsible for the pathogenesis of DN (6,7).

Histone deacetylation enzymes (HDACs) are a family of enzymes that are important in gene transcription and chromatin remodeling, with a dynamic balance between HDAC and histone acetyltransferase (HAT). HDACs can regulate cell proliferation, migration and death (8). Although the regulation of ERS is more complex, several studies have reported that histone acetylation modification can control the transcription of proteins involved in ERS (9-11).

Valproate (VPA) is a histone deacetylation enzyme inhibitor (HDACI) that increases the acetylation level of histones and promotes gene transcription. VPA has previously been used in antiepileptic and antitumor treatments. Currently, it has also been applied in the treatment of nerve degeneration, cardiovascular disease, autoimmune diseases and diabetes mellitus (12-14). VPA is now also suggested for the treatment of kidney disease; however, the therapeutic mechanism involved remains to be elucidated (15-17).

The present study aimed to determine whether VPA attenuates DN through the inhibition of ERS and the possible mechanism involved.

Materials and methods

Animals. All animal procedures were approved by the Institutional Animal Care and Use Committee of Jilin University and rats were handled in strict accordance with the guidelines of the care and use of medical laboratory animals

Correspondence to: Professor Lian-Kun Sun, Department of Pathophysiology, Basic College of Medicine, Jilin University, 126 Xinmin Street, Changchun, Jilin 130021, P.R. China
E-mail: sunlk@jlu.edu.cn

Key words: valproate, diabetic nephropathy, endoplasmic reticulum stress, histone acetylation, apoptosis

(Ministry of Health P.R. China, 2011) and the guidelines of the laboratory animal ethical standards of Jilin Medical University. A total of 60 adult male Wistar rats weighing 290±20 g and aged 8 weeks obtained from the Laboratory Animal Center of Jilin University (Changchun, China) were used in the present study. All animals received normal rat chow and tap water *ad libitum* in a constant environment (room temperature, 24±3˚C; room humidity, 55±5%) with a 12-h light/12-h dark cycle. The animals were kept under observation for 2 weeks prior to the start of the experiments.

Induction of a DN model and study design. A total of 60 Wistar rats were used in this experiment. For the normal control group, 20 rats were used (n=20), which received a single injection of 0.1 mol/l citrate buffer. A group of 40 rats were intravenously injected with streptozotocin (STZ; Sigma-Aldrich, St. Louis, MO, USA; 70 mg/kg body weight) in a 0.1 mol/l citrate buffer (pH 4.5). Only rats with blood glucose >11.1 mmol/l after 7 days were considered diabetic in the fasting state. Glucose measurement was performed using a OneTouch Select Analyzer (Roche Diagnostics GmbH, Mannheim, Germany). Rats with blood glucose <7.8 mmol/l were excluded from the study (6 rats). A total of 34 diabetic rats were fed a high-fat diet (45% kcal% fat) for 22 weeks. The normal control group was fed normal rat chow. During the 22 weeks, two diabetic rats died. In total, 32 diabetic rats were randomly divided into two groups: DN group (n=15) and the DN plus VPA treatment group (DN+VPA group; n=17). For the normal control group, 20 rats were also randomly divided into two groups: Normal group (N group; n=10) and normal plus VPA group (N+VPA group; n=10). Rats in the appropriate groups underwent intragastric administration of 200 mg/kg VPA (Sigma-Aldrich) in 50 μl of distilled water or 50 μl of distilled water alone once daily for 6 weeks. At week 6, all rats were euthanized. Body weight, blood glucose, plasma creatinine and 24-h urinary protein levels were measured regularly (fortnightly interval) and at the end of the experiment duration. Kidneys were dissected and rinsed with ice cold normal saline and then weighed. An index of renal hypertrophy was estimated by comparing the wet weight of the kidney to the body weight.

Urinary albumin assay. Urine samples were collected at the end of the experiment. Urine albumin (ELISA; IBL international GmbH, Hamburg, Germany) and blood creatinine (ELISA; BioVision Inc., San Francisco, CA, USA) were measured according to the manufacturer's instructions of the kits used.

Pathological examination. The kidney tissue of each group was collected, fixed with 40 g/l paraformaldehyde for 24 h, embedded in paraffin (Beyotime Institute of Biotechnology, Haimen, China) and sectioned at a thickness of 3-4 μm. The sections were deparaffinized and pathological changes were examined following hematoxylin (1 g hematoxylin dissolved in 100 ml distilled water) and eosin staining (Beyotime Institute of Biotechnology, Nanjing, China).

Transmission electron microscopy. The renal cortex was fixed in 2% glutaraldehyde in cacodylate buffer at 4˚C, postfixed in 1% osmium-tetroxide and stained with 2% uranyl acetate. The samples were dehydrated and embedded in Poly/bed 812 araldite resin (Polysciences Inc., Eppelheim, Germany). Ultrathin sections (50-100 nm) were cut with an ultramicrotome (Ultracut; Reichert-Jung, Depew, NY, USA), mounted on copper grids and examined with a Tecnai 10 transmission electron microscope (Philips, Eindhoven, Netherlands). Digital images were captured using a megaview G2 CCD camera (Soft Imaging System GmbH, Münster, Germany) at x6,200 magnification.

Immunohistochemical staining. The kidney tissue was fixed in 40 g/l paraformaldehyde for 24 h, embedded in paraffin, and then sectioned at a thickness of 3-4 μm. The sections were deparaffinized and 3% hydrogen peroxide in methanol was used to block endogenous peroxidase at room temperature for 30 min. Pre-incubation of sections for 30 min with 2% bovine serum albumin in 0.01 mol/l phosphate-buffered saline (PBS) was used to block nonspecific reactivity. The sections were then incubated with polyclonal rabbit anti-human GRP78 (ab21685), monoclonal mouse anti-human C/EBP homologous protein (CHOP; ab11419) or polyclonal rabbit anti-human caspase-12 antibodies at a dilution of 1:400 at 4˚C overnight [all antibodies were obtained from Abcam (Hong Kong) Ltd., Hong Kong]. The sections were washed with PBS, bound antibodies were detected with the SP1 kit (Beijing Zhongshan Golden Bridge Biotechnology Co., Ltd., Beijing, China) and immunoreactive products were visualized in 0.05% 3,3'-diaminobenzidine and 0.03% H_2O_2. The sections were counterstained with hematoxylin, dehydrated, cleared, counted and observed under an Olympus BX51 microscope (Olympus, Tokyo, Japan). In control staining, the sections were incubated with goat anti-mouse immunoglobulin G (IgG) [ab197767; Abcam (Hong Kong) Ltd.] instead of test antibodies.

Immunofluorescence staining. Sections of kidney tissue were prepared as described above. Following blocking with 3% normal goat serum in 0.1 M phosphate buffer containing 0.1% Triton X-100 (Sigma-Aldrich) for 30 min at room temperature, the sections were incubated with anti-GRP78, anti-CHOP or anti-caspase-12 antibodies [1:200; Abcam (Hong Kong) Ltd.] overnight at 4˚C. Following being washed with 0.1 M phosphate buffer, sections were reacted with Alexa Fluor 488-conjugated secondary antibody (1:400; Invitrogen; Thermo Fisher Scientific, Rockford, IL, USA) for 1 h, stained with Hoechst 33342 (2 μg/ml) for 2 min and washed with PBS three times. The sections were examined with a laser scanning confocal microscope (FV1000; Olympus) at an excitation wavelength of 488 nm.

Western blot analysis. Kidney tissues were homogenized in RIPA buffer (50 mM Tris-HCl, pH 7.5, 150 mM NaCl, 1 mM Na_2EDTA, 1 mM EDTA, 1% Triton, 2.5 mM sodium pyrophosphate, 1 mM β-glycerophosphate, 1 mM Na_3VO_4, 1 mM NaF, 1 μg/ml leupeptin and 1 mM PMSF; Beyotime Institute of Biotechnology) and total protein was extracted. The homogenized samples were boiled for 5 min and stored at -20˚C. The protein concentration was determined using a Pierce BCA kit (Thermo Fisher Scientific). For western blot analysis, protein lysates (30-50 μg) were resolved by 12% SDS-polyacrylamide gel electrophoresis (Beyotime Institute

of Biotechnology) and transferred onto immobilon-P transfer membranes (Millipore, Boston, MA, USA). The membranes were blocked with 5% non-fat milk powder in buffer [10 mM Tris-HCl, (pH 7.6), 100 mM NaCl and 0.1% Tween 20] for 2 h at room temperature and then incubated with the desired primary antibody, including polyclonal rabbit anti-human GPR78 (cat. no. ab21685), polyclonal rabbit anti-human caspase-12 (cat. no. ab4051), rabbit polyclonal anti-caspase-3, mouse anti-human monoclonal CHOP (cat. no. ab11419), monoclonal rat anti-human B-cell lymphoma 2 (Bcl-2; cat. no. ab166652), rabbit monoclonal anti-Bcl-2-associated X protein (Bax; cat. no. ab32503), polyclonal rabbit anti-phosphorylated JNK (pJNK; cat. no. ab4821), monoclonal mouse anti-activating transcription factor 4 (cat. no. ab23760) or monoclonal mouse anti-β-actin [cat. no. ab6276; 1:1,000 dilution; all obtained from Abcam (Hong Kong) Ltd.] overnight at 4˚C, followed by incubation with a horseradish peroxidase-conjugated secondary antibody (Hangzhou HuaAn Biotechnology Co., Ltd., Hangzhou, China) at a 1:2,000 dilution for 1.5 h at room temperature. The immunoreactive bands were visualized with 3,3'-diaminobenzidine (Sigma-Aldrich). The representative bands were measured by a Tanon GIS gel imager system (Tanon Science & Technology Co., Ltd., Shanghai, China) and analyzed. The levels of proteins were normalized to those of β-actin and the ratios are presented as the mean ± standard deviation of three independent experiments. Protein levels were quantified by densitometry using Quantity One 1-D software (version 4.4.02; Bio-Rad Laboratories, Hercules, CA, USA).

Terminal deoxynucleotidyl transferase dUTP nick end labeling (TUNEL). Analysis of apoptosis was performed using an In Situ Cell Death Detection kit (Roche Diagnostics, Indianapolis, IN, USA) to identify DNA breaks according to the manufacturer's instructions. Sections were incubated with the TUNEL reaction mix containing 10 units of terminal deoxyribosyltransferase, 10 mM dUTP-biotin and 2.5 mM cobalt chloride in 1X terminal transferase reaction buffer for 1 h at 37˚C in a humidified atmosphere. Apoptotic cells with characteristic nuclear fragmentation (staining green) were counted in six randomly selected fields. The experiment was repeated three times.

Chromatin immunoprecipitation assay (ChIP). ChIP assays using monoclonal rabbit anti-acetylated-histone H4 antibodies [ab109463; Abcam (Hong Kong) Ltd.] were performed to investigate the effects of VPA on the acetylation of histone in the GRP78 and CHOP promoter. ChIP assays were performed using a ChIP assay kit, according to the manufacturer's instructions (EMD Millipore, Billerica, MA, USA). Briefly, kidney tissues were treated as indicated and cross-linked with formaldehyde, then sonicated. Resulting kidney tissue lysates (input) were immunoprecipitated with anti-acetylated-histone H4 antibodies. The precipitated protein-DNA complexes (IP) were subjected to proteinase treatment. The following primers were used: GRP78, forward 5'-CTCGAGGAAGGGCATA AGAGCATCA-3' and reverse 5'-CCGCTTCTCCTCAGGTTC CGGCTGT-3'; CHOP, forward 5'-ACTGACAACGACAAG ACCCC-3' and reverse 5'-AGTCACAGCCAGTATCGAGC-3'; GAPDH, forward 5'-ACAACCTGGTCCTCAGTGTAGCC-3' and reverse 5'-AAGGTCATCCCAGAGCTGAACGG-3'.

Statistical analysis. Data are representative of three independent experiments, each conducted in triplicate. The differences between two groups were analyzed by the Kruskal-Wallis H non-parametric test using SPSS 19.0 for Windows (SPSS, Inc., Chicago, IL, USA). A two-sided P-value of $P<0.05$ was considered to indicate a statistically significant difference.

Results

VPA reduces ERS in a rat model of DN. Immunohistochemistry and immunofluorescence microscopy were used to determine the expression of the ERS-associated proteins GRP78, CHOP and caspase-12. Compared with the DN group, the expression of GRP78 in the DN+VPA group was enhanced, while the expression of CHOP and caspase-12 was reduced (Fig. 1A and B). Western blot analysis was used to quantify the expression of GRP78, CHOP and caspase-12. Similar to the immunohistology results, compared with the DN group, the expression of GRP78 in the DN+VPA group was enhanced, while the expression of CHOP and caspase-12 was significantly reduced (Fig. 1C and D). These results indicate that VPA can effectively reduce ERS in a rat model of DN.

VPA reduces apoptosis in a rat model of DN. The TUNEL assay was used to determine whether VPA could modulate apoptosis in kidney tissue in DN. Compared with the normal group, apoptosis was significantly increased in the DN group. However, compared with the DN group, apoptosis in the DN+VPA group was reduced following VPA treatment (Fig. 2A and B). Notably, apoptosis was predominantly concentrated in the renal tubules. Western blot analysis was then used to investigate the expression of apoptosis-associated proteins. Compared with the control group, the expression of pJNK, Bax and cleaved caspase-3 was enhanced in the DN group, while the expression of Bcl-2 protein was decreased. By contrast, compared with the DN group, the expression of pJNK, Bax and cleaved caspase-3 was reduced in the DN+VPA group, while the expression of Bcl-2 was enhanced (Fig. 2C and D). These results suggest that VPA reduces apoptosis in renal tissue.

VPA attenuates kidney injury in a rat model of DN. Excessive apoptosis eventually leads to organ dysfunction. Blood sugar, the ratio of kidney weight/body weight, serum creatinine and 24-h urinary protein were all significantly increased and body weight significantly reduced in the DN group compared with the normal group. However, compared with the DN group, in the DN+VPA group, 24-h urinary protein excretion and serum creatinine level were significantly reduced, while the blood sugar, body weight and kidney weight/body weight ratio exhibited no pronounced alterations (Fig. 3A-F). Histopathological changes were also examined. Compared with the normal group, in the DN group, the Bowman's space was decreased, the glomerular basement membrane was thickened, the mesangial matrix expanded and mesangial cells proliferated. Compared with the DN group, these pathological alterations were reduced in the DN+VPA group (Fig. 3G). Additionally, the ultrastructure of the kidney was observed using transmission electron microscopy. Compared with the normal group, the glomerular basement membrane became thickened, the structure of the membrane filtration layers was unclear, podocyte foot processes

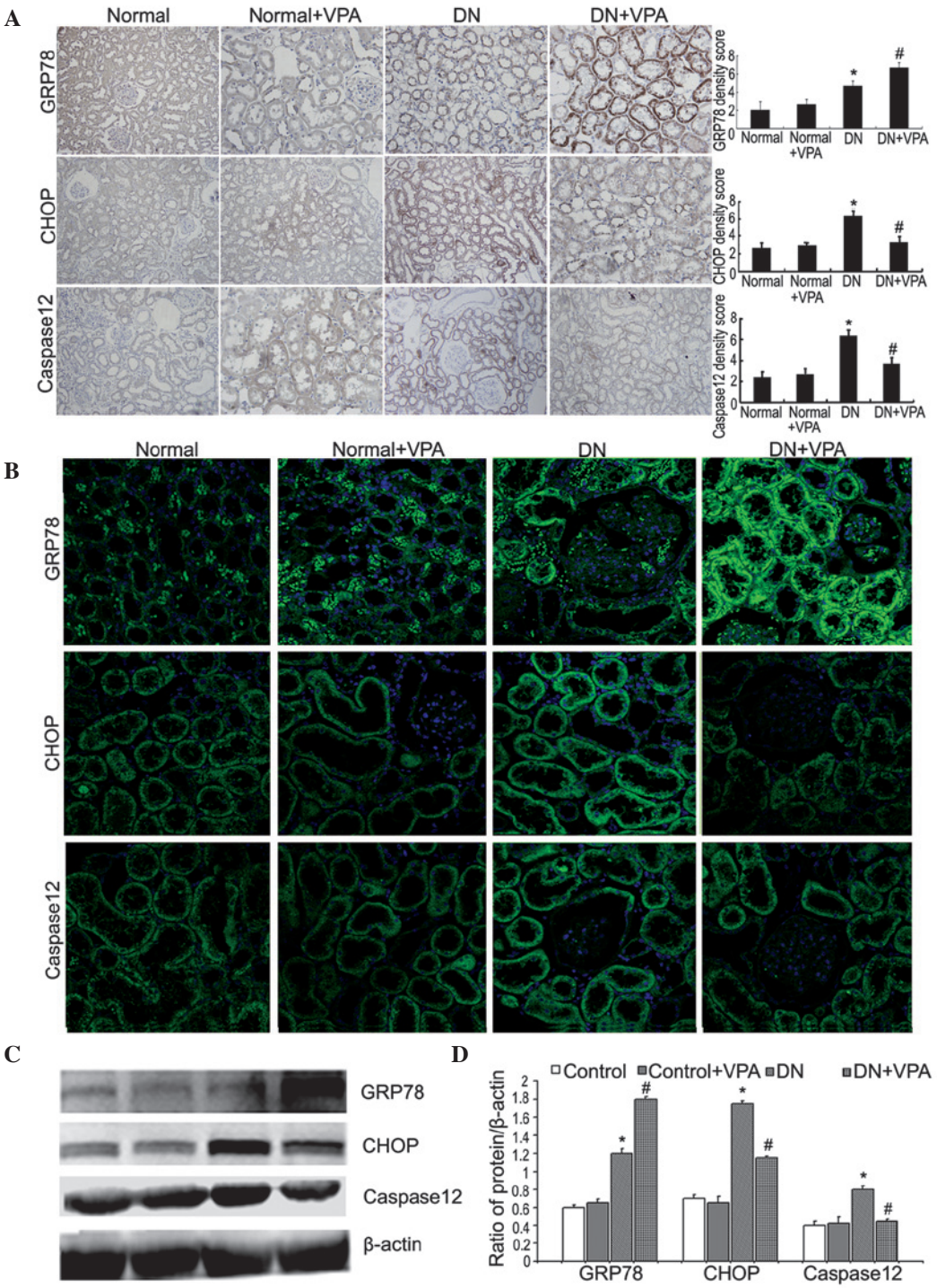

Figure 1. VPA relieves endoplasmic reticulum-stress-mediated apoptosis in DN rats. (A) Rats were divided into four groups: Normal group, normal+VPA group, DN group and the DN+VPA group. The kidney tissues removed from four groups were immunohistochemically stained with anti-GRP78, anti-CHOP and anti-caspase-12 antibody (top, magnification, x200). Quantitations of GRP78, CHOP and caspase-12 density score (bottom). Data are presented as the mean ± SD (n=3). *P<0.05 vs. the normal group; $^{\#}$P<0.05 vs. the DN group. (B) Expression levels of GRP78, CHOP and caspase-12 in kidney tissues removed from four groups were analyzed by confocal microscopy (magnification, x400). (C) Western blot analysis was used to analyze the expression of GRP78, CHOP and caspase-12 in kidney tissues removed from four groups (left). (D) Quantitations of GRP78, CHOP and caspase-12 protein levels (right). Data are presented as the mean ± SD (n=3). *P<0.05 vs. the normal group; $^{\#}$P<0.05 vs. the DN group. VPA, valproate; DN, diabetic nephropathy; SD, standard deviation; CHOP, C/EBP homologous protein; GRP78, glucose-regulated protein.

were disordered, the gap became broadened and the mesangial matrix was increased in the DN group. These findings were significantly attenuated in the DN+VPA group compared with the DN group (Fig. 3H), indicating that VPA can relieve renal injury in a rat model of DN.

VPA increases histone H4 acetylation in the GRP78 promoter and reduces histone H4 acetylation in the CHOP promoter. ChIP assay was used to detect the acetylation level of histone H4 in the GRP78 promoter. Compared with the normal group, the acetylation level of histone H4 in GRP78 was increased in the DN

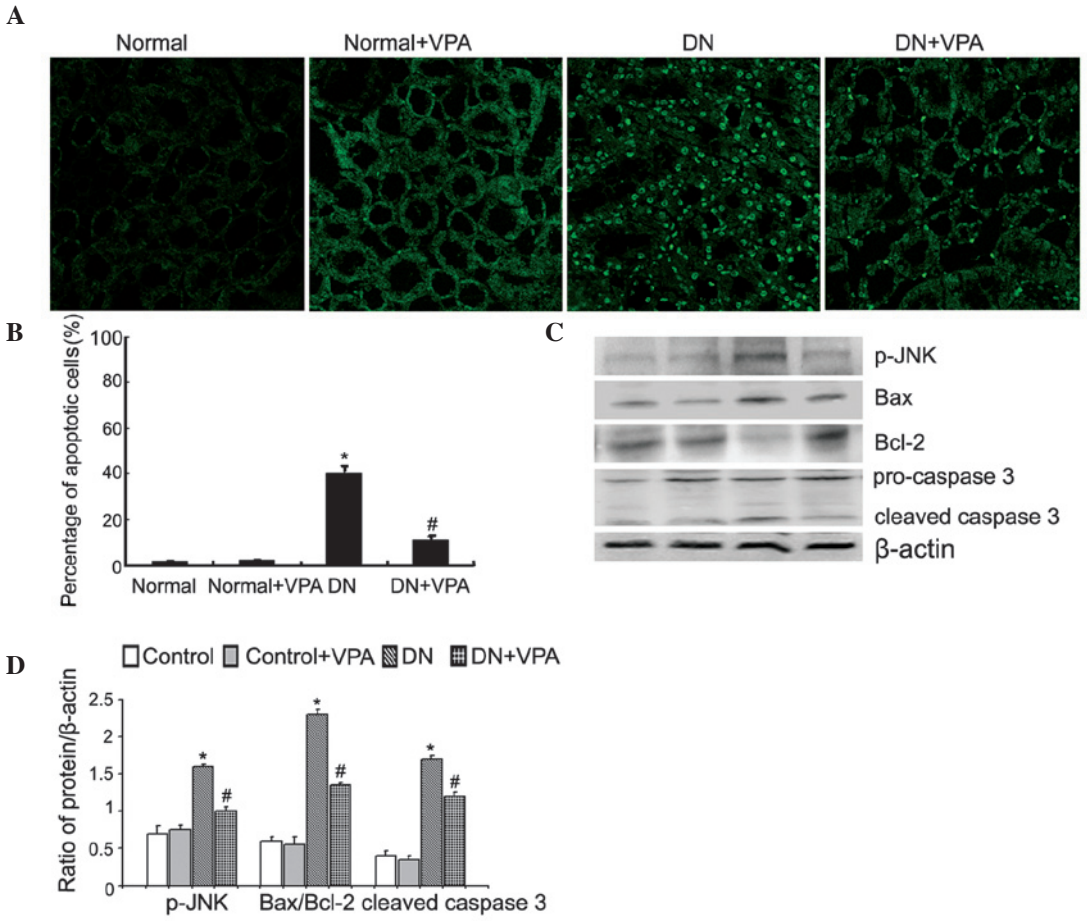

Figure 2. VPA reduces mitochondrial-mediated apoptosis in diabetic nephropathy rats. (A) Rats were divided into four groups: Normal group, normal+VPA group, DN group and the DN+VPA group. The kidney tissues removed from four groups were stained with TUNEL, followed by fluorescence microscopy at a magnification of x400 (top). (B) Quantitation of the percentage of apoptotic cells in four groups (bottom). Data are presented as the mean ± SD (n=3). *P<0.05 vs. the normal group; #P<0.05 vs. the DN group. (C) The expression of p-JNK, Bax, Bcl-2, procaspase-3 and cleaved caspase-3 in the four groups was investigated by western blot analysis (left). (D) Quantitation of p-JNK, Bax, Bcl-2, procaspase-3 and cleaved caspase-3 protein levels (right). Data are presented as the mean ± SD (n=3). *P<0.05 vs. the normal group; #P<0.05 vs. the DN group. VPA, valproate; DN, diabetic nephropathy; SD, standard deviation; Bax, Bcl-2-associated X protein; Bcl-2, B-cell lymphoma 2; p-JNK, phosphorylated JNK; TUNEL, terminal deoxynucleotidyl transferase dUTP nick end labeling.

group. The acetylation level of H4 in the GRP78 promoter was increased in the DN+VPA group compared with the DN group (Fig. 4A and B). The present study also assessed the acetylation level of H4 in the CHOP gene promoter. Compared with the DN group, the acetylation level of H4 in the CHOP gene promoter was reduced in the DN+VPA group (Fig. 4C and D). To determine why the acetylation of histone H4 in the CHOP promoter was altered, the protein expression of ATF4 was investigated, which is upstream of the CHOP gene. Compared with the normal group, the protein expression of ATF4 was increased in the DN group. However, the protein expression of ATF4 was reduced in the DN+VPA group compared with the DN group (Fig. 4E and F). These results indicated that VPA increases the acetylation level of histone H4 in the GRP78 promoter and reduces the acetylation level of histone H4 in the CHOP promoter.

Discussion

The functional role of the ER is the folding, modification and degradation of secretory and transmembrane proteins. Conditions, including oxidative stress, ischemia-reperfusion injury, hypoxia and calcium metabolism disorders can all induce ERS. ERS can lead to disorders of protein folding and cause the accumulation of unfolded and misfolded proteins. In order to restore ER homeostasis, a variety of cell signaling pathways are activated to maintain cell survival. However, when the stimulus inducing ERS persists, the ERS response eventually ends in apoptosis (5,7). Islet β-cells are particularly sensitive to alterations in the ER (18). High blood glucose, free fatty acids (19) and over-nutrition in diabetes mellitus are ERS-inducing factors. These factors can induce ERS in renal tubular epithelial cells or other renal cells (10,20), and if persistent may cause apoptosis (19,21). ERS can also lead to glomerular epithelial cell injury (22) with the subsequent proteinuria inducing ERS and apoptosis in renal tubular epithelial cells (23). Previous studies have indicated that suppression of the expression of the ERS-associated protein X-box binding protein 1 reduces fibrosis caused by kidney mesangial cells (24,25). Notably, Morse *et al* found that ERS was active in nephropathy (26). These data indicate that ERS is one mechanism involved in the pathogenesis of DN (7,21). In the present study, it was found that the expression of ERS-associated proteins GRP78, CHOP and caspase-12 were all significantly increased in DN. This suggests that apoptosis

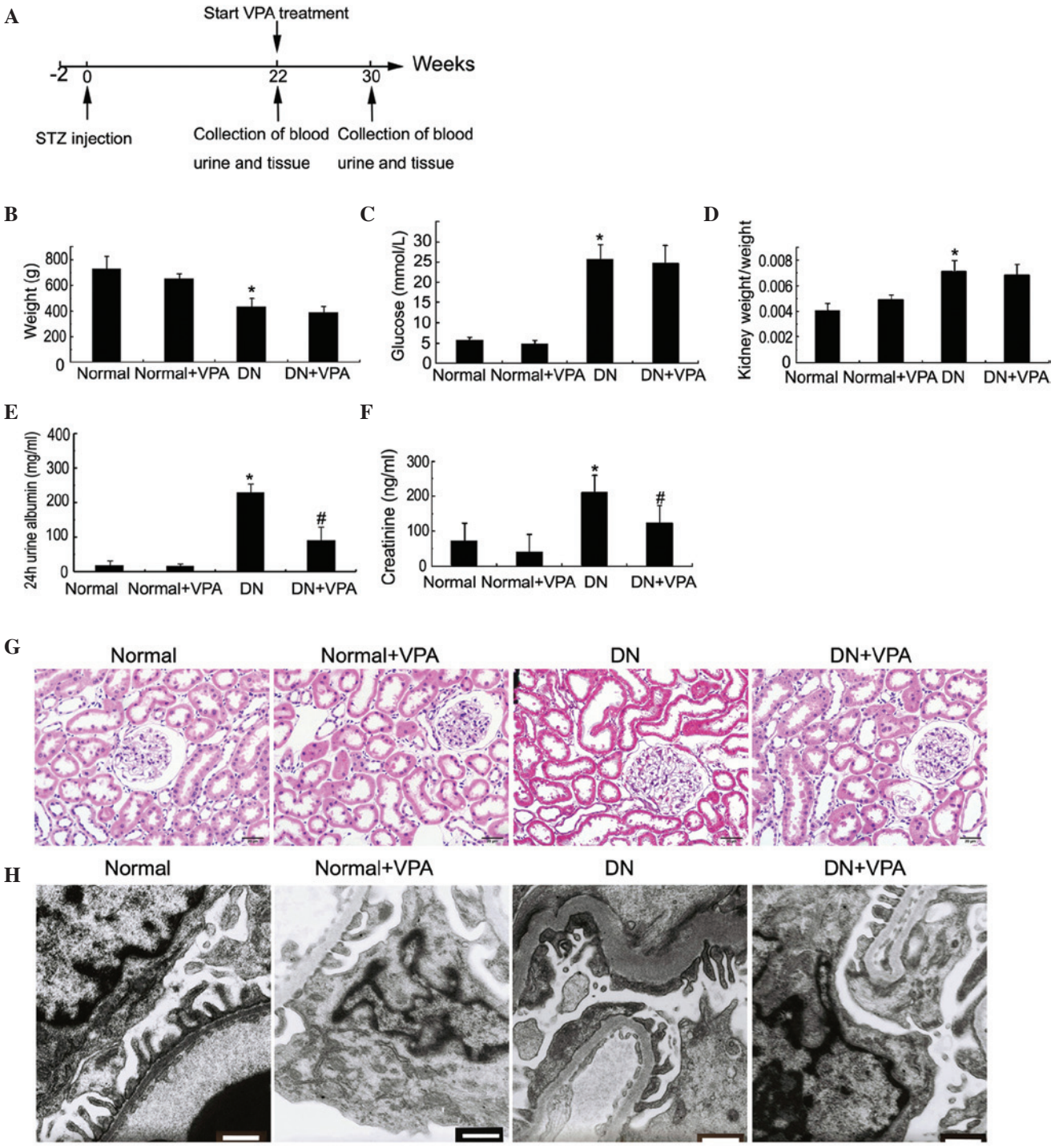

Figure 3. VPA relieves kidney injury in DN rats. (A) Different time points following STZ injection, VPA treatment and collection of blood urine and tissue. (B-F) Quantitation of weight, glucose, kidney weight/weight, 24 h urine albumin and creatinine in kidney tissues removed from four groups. Data are presented as the mean ± SD (n=3). *P<0.05 vs. the normal group; #P<0.05 vs. the DN group. (G) Immunohistochemistry was used to observe kidney tissues stained with hematoxylin and eosin in different groups (magnification, x400). (H) The ultrastructure of the kidney in different groups was observed by transmission electron microscope technology (scale bar=500 μm). VPA, valproate; DN, diabetic nephropathy; SD, standard deviation; STZ, streptozotocin.

in renal tissue in a rat model of DN is upregulated via an ERS-induced pathway.

The acetylation and deacetylation of histones is an important and common pathway in the regulation of gene expression. The dynamic balance between HDAC and HAT is critical in gene transcription and chromatin remodeling. Several studies have demonstrated that histone acetylation modification is associated with ERS (9,27). Zhang *et al* demonstrated that VPA increases the expression of GRP78 and reduces the expression of CHOP and caspase-12 by increasing the acetylation level of histone H3, attenuating retinal ischemia-reperfusion injury (27). Yu *et al* has demonstrated that trichostatin A (TSA), another HDACI, increases the expression of GRP78 in a myocardial ischemia-reperfusion injury model, and also reduces the expression of CHOP and caspase-12, therefore reducing apoptosis (9). In the present study, it was found that

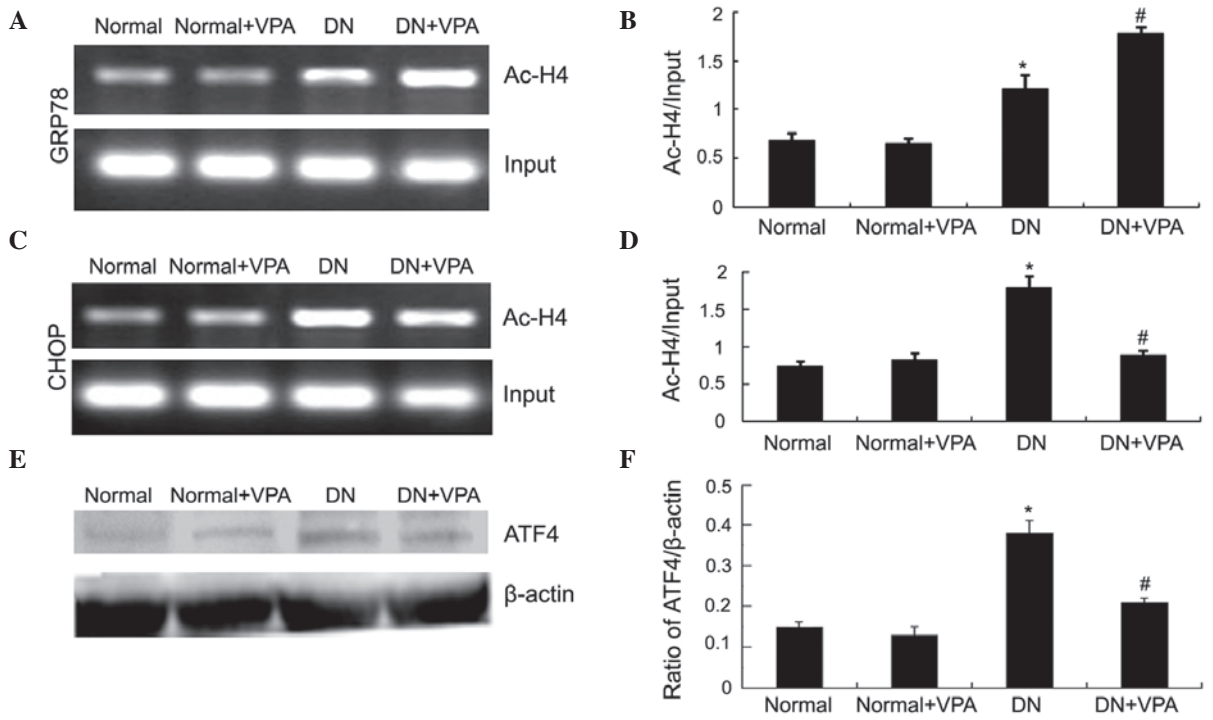

Figure 4. VPA increases the acetylation level of histone H4 in the GRP78 promoter and reduces the acetylation level of histone H4 in the CHOP promoter. (A) Acetylation level of histone H4 in the GRP78 promoter in kidney tissues removed from four groups was detected by ChIP assay. (B) Quantitation of the acetylation level of H4 in the GRP78 promoter. Data are presented as the mean ± SD (n=3). *P<0.05 vs. the normal group; #P<0.05 vs. the DN group. (C) The acetylation level of histone H4 in the CHOP promoter in kidney tissues removed from four groups was detected by ChIP assay. (D) Quantitation of the acetylation level of H4 in the CHOP promoter. Data are presented as the mean ± SD (n=3). *P<0.05 vs. the normal group; #P<0.05 vs. the DN group. (E) Western blot analysis of ATF4 in kidney tissues removed from four groups. (F) Quantitation of ATF4 protein levels. Data are presented as the mean ± SD (n=3). *P<0.05 vs. the normal group; #P<0.05 vs. the DN group. VPA, valproate; DN, diabetic nephropathy; SD, standard deviation; GRP78, glucose-regulated protein; CHOP, C/EBP homologous protein; ChIP, chromatin immunoprecipitation; ATF4, activating transcription factor 4.

VPA increases the expression of GRP78 and reduces the expression of CHOP and caspase-12 and decreases apoptosis in a rat model of DN. This suggests that VPA can relieve ERS in DN and thus decrease ERS-induced apoptosis. It was also found that 24-h urinary protein excretion and serum creatinine were reduced in the DN+VPA group compared with the DN group. Kidney histopathology and ultrastructure were also improved, thus VPA can also attenuate overall renal injury in DN.

In order to elucidate how VPA regulates ERS, the present study further investigated the acetylation level of histone H4 in ERS-associated protein promoters. The acetylation level of histone H4 in the GRP78 promoter was increased in the DN+VPA group, suggesting that VPA can inhibit HDAC indirectly to increase the acetylation level of histones in the GRP78 gene promoter H4, which promotes the transcription of the GRP78 gene. Baumeister *et al* reported that ERS-induced binding of the histone acetyltransferase p300 to the GRP78 promoter and histone H4 acetylation of the ER-bound bZIP family transcription factor is activated upon ERS, inducing histone H3 and H4 acetylated promoter gene transcription (28). The acetylation of histone H3 and H4 in the activating transcription factor 6α (ATF6α) promoter regulates ATF6α gene transcription (29). These data indicate that histone acetylated modification is associated with ERS. Bown *et al* also found that VPA can regulate the transcription of ERS-associated proteins (30). Following ERS induction, SGF29 is required for increased H3K14 acetylation in the ERS genes GRP78 and CHOP promoters, which then results in full transcriptional activation (11). This suggests HDACI may be associated with the level of histone H3 and H4 acetylation in ERS-targeted protein promoters. It was found that VPA can increase the acetylation of histone H4 in the GRP78 promoter, which promotes the protein expression of GRP78. Notably, it was found that VPA reduces the acetylation of histone H4 in the CHOP promoter. Yu *et al* found that TSA can also reduce the acetylation of histone H3 in the CHOP promoter in myocardial ischemia-reperfusion injury (9). Shan *et al* found that following amino acid deprivation, a primary function of ATF4 was to recruit HAT to target genes. ATF4 bound to the genes prior to histone acetylation, thus ATF4 functions as a pioneering factor to alter chromatin structure to enhance transcription in a gene-specific manner (31). ATF4 is upstream of the CHOP gene and is also the main transcription factor promoting CHOP gene transcription. Fawcett *et al* identified that ATF4 can bind to the CHOP gene promoter at C/EBP-ATF sites to promote CHOP mRNA expression in arsenite-treated PC12 cells (32). In the present study, it was found that VPA reduces the protein expression of ATF4 in the DN+VPA group. Therefore, it was hypothesized that VPA may reduce the expression of ATF4, through inhibition of the binding of ATF4 to the CHOP promoter, thereby inhibiting the recruitment of HAT and eventually decreasing the acetylation of histone H4 in the CHOP promoter.

In conclusion, the present study demonstrated that VPA can relieve ERS in a rat model of DN and reduces ERS-induced

apoptosis, thereby attenuating diabetes-induced renal injury. This may be performed through the regulation of histone H4 acetylation in the promoters of the ERS-associated proteins GRP78 and CHOP. These results provide initial experimental evidence for the treatment of DN with VPA.

Acknowledgements

The authors would like to thank Professor Lining Miao and Dr Yangwei Wang from the Second Clinical Hospital of Jilin University for their assistance with the animal models, and Mr. Liwen Bianji (Edanz Group China) for the editing of the manuscript.

References

1. Grace BS, Clayton P and McDonald SP: Increases in renal replacement therapy in Australia and New Zealand: Understanding trends in diabetic nephropathy. Nephrology (Carlton) 17: 76-84, 2012.
2. Maric C and Hall JE: Obesity, metabolic syndrome and diabetic nephropathy. Contrib Nephrol 170: 28-35, 2011.
3. Giacco F and Brownlee M: Oxidative stress and diabetic complications. Circ Res 107: 1058-1070, 2010.
4. Ozcan U, Cao Q, Yilmaz E, Lee AH, Iwakoshi NN, Ozdelen E, Tuncman G, Görgün C, Glimcher LH and Hotamisligil GS: Endoplasmic reticulum stress links obesity, insulin action, and type 2 diabetes. Science 306: 457-461, 2004.
5. Higa A and Chevet E: Redox signaling loops in the unfolded protein response. Cell Signal 24: 1548-1555, 2012.
6. Cao Y, Hao Y, Li H, Liu Q, Gao F, Liu W and Duan H: Role of endoplasmic reticulum stress in apoptosis of differentiated mouse podocytes induced by high glucose. Int J Mol Med 33: 809-816, 2014.
7. Cunard R and Sharma K: The endoplasmic reticulum stress response and diabetic kidney disease. Am J Physiol Renal Physiol 300: F1054-F1061, 2011.
8. Choudhary C, Kumar C, Gnad F, Nielsen ML, Rehman M, Walther TC, Olsen JV and Mann M: Lysine acetylation targets protein complexes and co-regulates major cellular functions. Science 325: 834-840, 2009.
9. Yu L, Lu M, Wang P and Chen X: Trichostatin A ameliorates myocardial ischemia/reperfusion injury through inhibition of endoplasmic reticulum stress-induced apoptosis. Arch Med Res 43: 190-196, 2012.
10. Zhang X, Zhao Y, Chu Q, Wang ZY, Li H and Chi ZH: Zinc modulates high glucose-induced apoptosis by suppressing oxidative stress in renal tubular epithelial cells. Biol Trace Elem Res 158: 259-267, 2014.
11. Schram AW, Baas R, Jansen PW, Riss A, Tora L, Vermeulen M and Timmers HT: A dual role for SAGA-associated factor 29 (SGF29) in ER stress survival by coordination of both histone H3 acetylation and histone H3 lysine-4 trimethylation. PloS One 8: e70035, 2013.
12. Kim HJ, Rowe M, Ren M, Hong JS, Chen PS and Chuang DM: Histone deacetylase inhibitors exhibit anti-inflammatory and neuroprotective effects in a rat permanent ischemic model of stroke: Multiple mechanisms of action. J Pharmacol Exp Ther 321: 892-901, 2007.
13. Ren M, Leng Y, Jeong M, Leeds PR and Chuang DM: Valproic acid reduces brain damage induced by transient focal cerebral ischemia in rats: Potential roles of histone deacetylase inhibition and heat shock protein induction. J Neurochem 89: 1358-1367, 2004.
14. Wang Z, Leng Y, Tsai LK, Leeds P and Chuang DM: Valproic acid attenuates blood-brain barrier disruption in a rat model of transient focal cerebral ischemia: The roles of HDAC and MMP-9 inhibition. J Cereb Blood Flow Metab 31: 52-57, 2011.
15. Van Beneden K, Geers C, Pauwels M, Mannaerts I, Verbeelen D, van Grunsven LA and Van den Branden C: Valproic acid attenuates proteinuria and kidney injury. J Am Soc Nephrol 22: 1863-1875, 2011.
16. Noh H, Oh EY, Seo JY, Yu MR, Kim YO, Ha H and Lee HB: Histone deacetylase-2 is a key regulator of diabetes- and transforming growth factor-beta1-induced renal injury. Am J Physiol Renal Physiol 297: F729-F739, 2009.
17. Advani A, Huang Q, Thai K, Advani SL, White KE, Kelly DJ, Yuen DA, Connelly KA, Marsden PA and Gilbert RE: Long-term administration of the histone deacetylase inhibitor vorinostat attenuates renal injury in experimental diabetes through an endothelial nitric oxide synthase-dependent mechanism. Am J Pathol 178: 2205-2214, 2011.
18. Song B, Scheuner D, Ron D, Pennathur S and Kaufman RJ: Chop deletion reduces oxidative stress, improves beta cell function, and promotes cell survival in multiple mouse models of diabetes. J Clin Invest 118: 3378-3389, 2008.
19. Tao JL, Wen YB, Shi BY, Zhang H, Ruan XZ, Li H, Li XM, Dong WJ and Li XW: Endoplasmic reticulum stress is involved in podocyte apoptosis induced by saturated fatty acid palmitate. Chin Med J (Engl) 125: 3137-3142, 2012.
20. Anil Kumar P, Welsh GI, Saleem MA and Menon RK: Molecular and cellular events mediating glomerular podocyte dysfunction and depletion in diabetes mellitus. Front Endocrinol (Lausanne) 5: 151, 2014.
21. Qi W, Mu J, Luo ZF, Zeng W, Guo YH, Pang Q, Ye ZL, Liu L, Yuan FH and Feng B: Attenuation of diabetic nephropathy in diabetes rats induced by streptozotocin by regulating the endoplasmic reticulum stress inflammatory response. Metabolism 60: 594-603, 2011.
22. McAlpine CS, Bowes AJ and Werstuck GH: Diabetes, hyperglycemia and accelerated atherosclerosis: Evidence supporting a role for endoplasmic reticulum (ER) stress signaling. Cardiovasc Hematol Disord Drug Targets 10: 151-157, 2010.
23. Lindenmeyer MT, Rastaldi MP, Ikehata M, Neusser MA, Kretzler M, Cohen CD and Schlöndorff D: Proteinuria and hyperglycemia induce endoplasmic reticulum stress. J Am Soc Nephrol 19: 2225-2236, 2008.
24. Kimura K, Jin H, Ogawa M and Aoe T: Dysfunction of the ER chaperone BiP accelerates the renal tubular injury. Biochem Biophys Res Commun 366: 1048-1053, 2008.
25. Shao D, Liu J, Ni J, Wang Z, Shen Y, Zhou L, Huang Y, Wang J, Xue H, Zhang W and Lu L: Suppression of XBP1S mediates high glucose-induced oxidative stress and extracellular matrix synthesis in renal mesangial cell and kidney of diabetic rats. PloS One 8: e56124, 2013.
26. Morse E, Schroth J, You YH, Pizzo DP, Okada S, Ramachandrarao S, Vallon V, Sharma K and Cunard R: TRB3 is stimulated in diabetic kidneys, regulated by the ER stress marker CHOP, and is a suppressor of podocyte MCP-1. Am J Physiol Renal Physiol 299: F965-F972, 2010.
27. Zhang Z, Tong N, Gong Y, Qiu Q, Yin L, Lv X and Wu X: Valproate protects the retina from endoplasmic reticulum stress-induced apoptosis after ischemia-reperfusion injury. Neurosci Lett 504: 88-92, 2011.
28. Baumeister P, Luo S, Skarnes WC, Sui G, Seto E, Shi Y and Lee AS: Endoplasmic reticulum stress induction of the Grp78/BiP promoter: Activating mechanisms mediated by YY1 and its interactive chromatin modifiers. Mol Cell Biol 25: 4529-4540, 2005.
29. Misra J, Kim DK, Choi W, Koo SH, Lee CH, Back SH, Kaufman RJ and Choi HS: Transcriptional cross talk between orphan nuclear receptor ERRγ and transmembrane transcription factor ATF6α coordinates endoplasmic reticulum stress response. Nucleic Acids Res 41: 6960-6974, 2013.
30. Bown CD, Wang JF, Chen B and Young LT: Regulation of ER stress proteins by valproate: Therapeutic implications. Bipolar Disord 4: 145-151, 2002.
31. Shan J, Fu L, Balasubramanian MN, Anthony T and Kilberg MS: ATF4-dependent regulation of the JMJD3 gene during amino acid deprivation can be rescued in Atf4-deficient cells by inhibition of deacetylation. J Biol Chem 287: 36393-36403, 2012.
32. Fawcett TW, Martindale JL, Guyton KZ, Hai T and Holbrook NJ: Complexes containing activating transcription factor (ATF)/cAMP-responsive-element-binding protein (CREB) interact with the CCAAT/enhancer-binding protein (C/EBP)-ATF composite site to regulate Gadd153 expression during the stress response. Biochem J 339: 135-141, 1999.